ISBN: 978-3-95450-247-9 ISSN: 2673-5490 doi: 10.18429/JACoW-IPAC2024-WEPG22

SLICE ENERGY SPREAD MEASUREMENTS OF A 20 MeV ELECTRON BEAM AT PITZ

C. Richard*, P. Boonpornprasert, D. Dmytriiev, M. Gross, A. Hoffmann, M. Krasilnikov, X.-K. Li, F. Stephan, G. Vashchenko, Deutsches Elektronen-Synchrotron DESY, Zeuthen, Germany

Abstract

Due to improvements of the performance of FELs, the measurements of the beam's slice energy spread is becoming increasingly important for optimization of the brightness. Of particular interest are measurements of the uncorrelated energy spread near the gun as this determines the lower limit of the energy spread for the rest of the machine. At the Photo Injector Test facility at DESY in Zeuthen (PITZ), the uncorrelated energy spread is measured of an electron beam generated from an L-band electron gun and accelerated to 20 MeV with a booster cavity. The energy spread of the central time slice is measured using a transverse deflecting structure (TDS) and a dispersive arm to image the longitudinal phase space. Scans of the TDS voltage and quadrupole strengths are used to remove the contributions from the TDS, transverse emittance, and imaging resolution. Presented is an overview of the measurement procedure, resolution, and results of measurements tests.

INTRODUCTION

The slice energy spread (SES) of electron beams is becoming increasingly important for optimizing the brightness of free electron lasers (FELs). If the SES is too large, then lasing isn't possible, but if it is too small then the beam can be destroyed by the microbunching instability. There are multiple methods to measure the SES including optimizing of the optical klystron effect [1], coherent harmonic generation [2], and dispersive measurements [3]. Most of these measurements are done at high energy, >100 MeV, to study the SES of the lased beam. However, it is also of interest to study the SES of low energy beams near the gun as this defines the initial conditions for studying the evolution of the SES along the beamline and determining the required performance for devices such as laser heaters [4].

The Photo Injector Test Facility at DESY in Zeuthen (PITZ) is an excellent beamline for measuring SES at low energy. PITZ commissions and characterizes electron guns for use in FELs at FLASH and European XFEL [5]. It is capable of generating 1 pC through 4 nC beams and typical final momentum of 17-22 MeV/c. Because the primary use of PITZ is beam characterization, it has a large suite of diagnostics including three dispersive arms (one at low energy and two at high energy), three slit stations for measuring emittance, an RF transverse deflecting structure (TDS), and multiple sciltinating screen stations for profile measurements. Using the existing infrastructure, the SES has beam measured at PITZ using the TDS and downstream dispersive arm to directly image the longitudinal phase space (LPS) [6].

* christopher.richard@desy.de

Systematic Errors

Slice energy spread is small and tends to be near the resolution limit of the imaging system. Therefore care must be taken to remove the systematic contributions. The measured SES is given by

$$\sigma^2_{E,\mathrm{meas}} = \sigma^2_E + \sigma^2_{E,\mathrm{TDS}} + \left(\frac{D}{E}\sigma_{\mathrm{im}}\right)^2 + \left(\frac{D}{E}\sigma_\perp\right)^2 \quad (1)$$

where $\sigma_{E,\mathrm{meas}}$ is the measured SES, σ_E is the true SES, $\sigma_{E,\mathrm{TDS}}$ is the energy spread added from the TDS, D is the dispersion, E is the mean beam energy, σ_{im} is the imaging resolution, and $\sigma_\perp$ is the contribution from the transverse emittance [7]. The TDS contribution is proportional to the TDS voltage and is accounted for by measuring the SES at multiple TDS voltages and fitting to

$$\sigma^2_{E,\mathrm{meas}} = \sigma^2_0 + \sigma^2_{E,\mathrm{TDS}} = \sigma^2_0 + (A \cdot V_{\mathrm{TDS}})^2 \quad (2)$$

where σ_0 contains all the non-TDS components.

A common method of accounting for σ_{im} and $\sigma_\perp$ is to scan the energy or dispersion and fit the measured SES [3]. For the low energy measurements at PITZ, this is not possible because it significantly changes the space charge forces which changes the true SES. Instead, at PITZ, these two contributions are measured separately [6]. However, the advantage of low energy measurements is improved energy resolution.

Beamline Setup

The PITZ beamline used for SES measurements is shown in Figure 1. For these measurements, the 1.3 GHz photo-gun produced a 250 pC beam at beam momentum of 6.0 MeV/c which was then accelerated to 20 MeV/c in the CDS booster. The beam is transported through the TDS for temporal streaking in the vertical plane then into a horizontal dispersive arm with dispersion $D = 0.9$ m for energy resolution. The resulting beam distribution is then recorded on a LYSO scintillating screen (Fig. 2). The booster phase is then adjusted to minimize the x-y coupling on the screen. Assuming the transverse emittance is small enough, the measured distribution is the longitudinal phase space of the beam. To reduce the contribution of the transverse emittance, a slit (slit 1 in Fig. 1) is inserted before the dipole to cut the beam in the dispersive plane. A slit (slit 2 in Fig. 1) is inserted before the TDS to reduce the beam size in the TDS to reduce the energy spread added by the TDS. Quadrupoles before the TDS are used for transport and an additional quadrupole after the second slit is used to vary R_{12} between the slit and the screen.

ISBN: 978-3-95450-247-9 ISSN: 2673-5490 doi: 10.18429/JACoW-IPAC2024-WEPG22

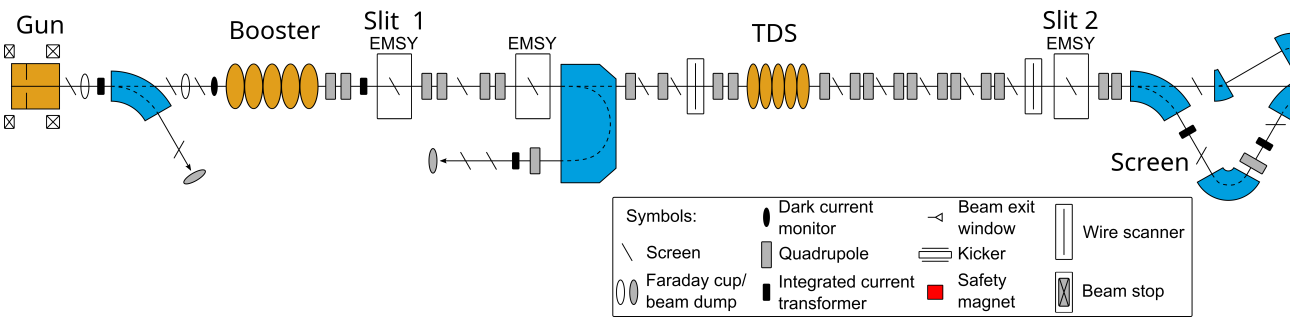

Figure 1: Sketch of SES measurement setup at PITZ.

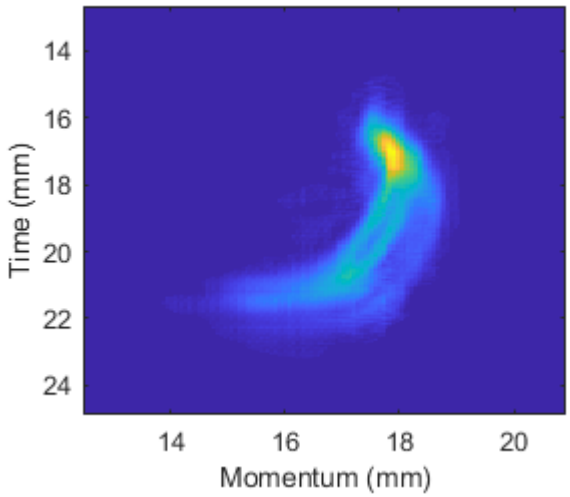

Figure 2: Example measured longitudinal phase space in the dispersive arm.

DETERMINING THE IMAGING RESOLUTION

While bench measurements were taken to measure the resolution of the imaging system, the results can be sensitive to the exact positioning of the lens and camera. Therefore, the resolution of the system is measured using the beam. This is done inserting a slit before the dipole to cut in the non-dispersive plane then scanning a quadrupole to vary R_{12} between the slit and the screen. R_{12} can be measured by scanning a steerer magnet and measuring the change in position at the screen. Assuming a thin lens quadrupole with strength κ the transport matrix between the kicker and screen is

$$R_{\text{k-s}} = \begin{bmatrix} 1+\kappa L_3 & (L_2+L_3)+\kappa L_2 L_3 \\ \kappa & 1 \end{bmatrix} \tag{3}$$

Where L_2 is the drift length between the steerer and the quadrupole and L_3 is the drift length between the quadrupole and screen. This can be rewritten in terms of the measured R_{12}

$$R_{\text{k-s}} \equiv \begin{bmatrix} \frac{R_{12}-L_3}{L_2} & R_{12} \\ \frac{R_{12}-L_2-L_3}{L_2 L_3} & \frac{R_{12}-L_2}{L_3} \end{bmatrix}. \tag{4}$$

By multiplying by a drift matrix from the screen to the kicker of length L_1, $R_{12,\text{sl-s}}$ between the slit and the screen is

$$R_{12,\text{sl-s}} = \frac{(L_1+L_2)R_{12} - L_1 L_3}{L_2}. \tag{5}$$

Due to the inserted slit, the beam size on the screen is dominated by the initial rms angle and the beam size at the screen is

$$\sigma_{x,f} = \sqrt{\sigma_{\text{im}}^2 + R_{12,\text{sl-s}}^2 \sigma_{x',i}^2}. \tag{6}$$

The screen resolution can then be determined by varying a quadrupole to change R_{12} and the beam size then fitting to

$$\sigma_x = \sqrt{\sigma_{\text{im}}^2 + a(R_{12}-b)^2}. \tag{7}$$

The imaging resolution was measured to be 85.3 ± 0.9 µm (Fig. 3).

Future Imaging Improvements

One of the primary challenges with SES measurements at PITZ is the short pulse length of the TDS RF system which limits the number of streaked bunches to only three per pulse. The limited number of bunches in combination with the two slits and strong streaking cause the measurements to be close to the noise floor. This has been partially alleviated with an installation of a new photocathode laser which has a higher repetition rate, 4.5 MHz, compared to the previous laser, 1 MHz [8]. This allows 13 bunches to be streaked by the TDS.

Another challenge at PITZ is the resolution of imaging optics relies on an f80 lens (focal length of 80 mm) for focusing. This lens was chosen because the lens can be placed close to the screen to increase the signal and also view the entire screen. However, the resolution of this lens is dominated by the spherical aberrations. In order to improve the resolution to accurately measure the SES, the aperture on the lens needed to be reduced. However, this comes at the cost of the already limited signal.

ISBN: 978-3-95450-247-9 ISSN: 2673-5490 doi: 10.18429/JACoW-IPAC2024-WEPG22

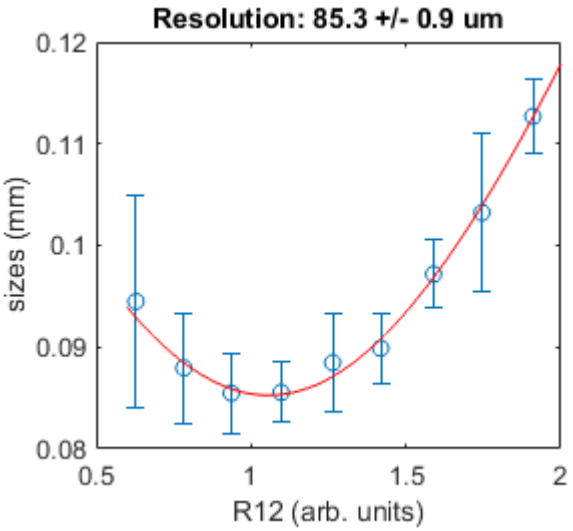

Figure 3: R12 scan in non-dispersive plane to determine the imaging resolution. Fitting to Eq. 3 with $\sigma_{\text{im}} = 85.2$ µm, a=0.086, b=-0.09.

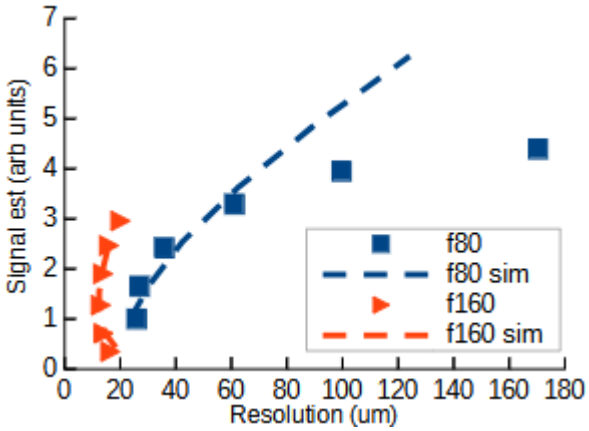

Figure 4: Signal and resolution comparison of the f80 and f160 lenses for aperture diameters from 10 to 25 mm in 3 mm steps. The f160 outperforms the f80 in signal and resolution.

To alleviate this issue, the lens can be changed to one with a longer focal length while keeping the position the same. Figure 4 shows the results of Zemax [9] simulations and bench tests of the resolution with an f80 and f160 lens. With the f160 lens, the resolution is significantly less dependent on the aperture. Therefore it can be fully opened, 25 mm diameter, to get better signal and still have better resolution than the f80 lens.The downside of the f160 lens is the reduced object area. The f80 lens was originally chosen because it views the full 38 mm LYSO screen so the full beam can be seen with strong streaking from the TDS. The f160 lens can only view approximately 15 mm and the edges of the beam are not seen with strong streaking. This is not an issue for SES measurements because it is only required to image a slice near the center of the beam where the energy-time coupling is minimized.

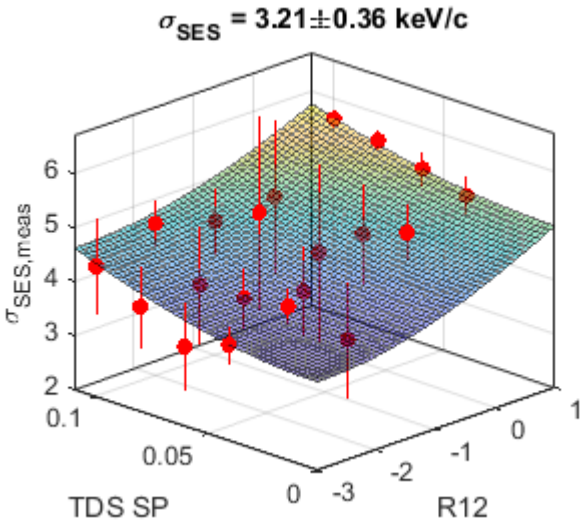

Figure 5: Scan of TDS voltage and R12 to measure the SES. The measured energy spreads are fit to Eq. 8 to determine the SES of the beam with σ_{SES}=3.21, a=0.87, b=2.92, c=25.76.

SES MEASUREMENTS

The remaining two components of the SES are removed by scanning the relevant parameters. Previously at PITZ, $\sigma_\perp$ was measured for a single R_{12} by turning off the dipole to measure the rms angle of the beamlet then the TDS voltage was scanned. To improve the accuracy of the measurements, the $\sigma_\perp$ component is now removed by scanning R_{12} similar to the screen resolution measurements, but in the dispersive plane. In addition the TDS voltage is scanned to account for $\sigma_{E,\text{TDS}}$. This 2D scan further reduces the SNR and is only possible due to the higher repetition rate of the new laser. These two parameters are scanned in a single two dimensional scan and the measured energy spreads can then be fit to

$$\sigma_{\text{SES, meas}} = \sqrt{\sigma_{\text{SES}}^2 + \sigma_{\text{res}}^2 + a(R_{12} - b)^2 + (cV_{\text{TDS}})^2} \quad (8)$$

to determine the true slice energy spread (Fig. 5). The measured SES was 3.21 ± 0.36 keV/c.

The slice energy spread is measured at each point by dividing the imaged longitudinal phase space into time slices. Each slice is fit to a Gaussian to determine the energy spread and the SES is defined as the minimum energy spread of the slices. This typically occurs at the center of the beam where there is no energy-time coupling.

OUTLOOK

Measurements of the SES at PITZ are improving. The new 4.5 MHz laser system significantly improves the SNR. This allows for 2D TDS voltage and R12 scans to further improve the measurement reliability. In addition, work is being done to improve the imaging setup to increase the resolution. With these improvements, future measurements are planned to study the behavior of the SES over a range of photogun settings.

ISBN: 978-3-95450-247-9 ISSN: 2673-5490 doi: 10.18429/JACoW-IPAC2024-WEPG22

REFERENCES

[1] E. Prat *et al.*, "Using the optical-klystron effect to increase and measure the intrinsic beam energy spread in free-electron-laser facilities", *Phys. Rev. Accel. Beams*, vol. 20, no. 4, Apr. 2017. doi:10.1103/physrevaccelbeams.20.040702

[2] C. Feng *et al.*, "Measurement of the average local energy spread of electron beam via coherent harmonic generation", *Phys. Rev. Spec. Top. Accel Beams*, vol. 14, no. 9, Sep. 2011. doi:10.1103/physrevstab.14.090701

[3] S. Tomin *et al.*,"Accurate measurement of uncorrelated energy spread in electron beam", *Phys. Rev. Accel. Beams*, vol. 24, no. 6, Jun. 2021. doi:10.1103/physrevaccelbeams.24.064201

[4] Z. Huang and K.-J. Kim, "Review of x-ray free-electron laser theory", *Phys. Rev. Spec. Top. Accel Beams*, vol. 10, no. 3, Mar. 2007. doi:10.1103/physrevstab.10.034801

[5] M. Krasilnikov *et al.*, "Experimentally minimized beam emittance from an *L*-band photoinjector", *Phys. Rev. Spec. Top. Accel Beams*, vol. 15, no. 10, Oct. 2012. doi:10.1103/physrevstab.15.100701

[6] H. Qian *et al.*, "Slice energy spread measurement in the low energy photoinjector", *Phys. Rev. Accel. Beams*, vol. 25, no. 8, Aug. 2022. doi:10.1103/physrevaccelbeams.25.083401

[7] K. Floettmann, V. Paramonov, "Beam dynamics in transverse deflecting rf structures", *Phys. Rev. Spec. Top. Accel Beams*, vol. 17, no. 2, Feb. 2014. doi:10.1103/physrevstab.17.024001

[8] Y. Chen *et al.*, "Characterization of low-emittance electron beams generated by a new photocathode drive laser system NEPAL at the European XFEL", presented at the IPAC'24, Nashville, TN, USA, May 2024, paper MOPG47, this conference.

[9] Ansys Zemax OpticsStudio 2023.